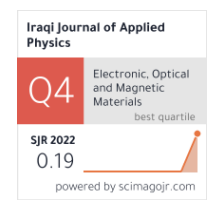
Ihal A. Abed Basma I. Waisi

Department of Chemical Engineering, College of Engineering, University of Baghdad, Baghdad, IRAQ



Preparation and Characterization of PES Flat Sheet Membrane Embedded with PEG for Dye Filtration Application

Membrane systems are widely regarded as a viable and sustainable method for removing colors from wastewater. The present work investigates the enhancement of prepared polyethersulfone polymer (PES) by embedding polyethylene glycol (PEG) polymer using phase inversion method. The polymer content was maintained at 16 wt.%. The present study investigated the impact of adding the PEG on the permeability flow and percentage of removal of Malachite Green dyes. The content and structure of the membrane were characterized. The dye concentration in the solution was measured to be 10 ppm under a pressure of 6 bar and thickness of 150 µm. The examination involved the analysis of PEG polymers with varying weight percentages (5, 10, and 15 wt.%). The optimal concentration of PEG polymer in the ultrafiltration membrane is determined based on factors such as casting solution composition, mechanical properties of the membrane, microstructures, water flux, and dye removal. In this case, it has been found that a concentration of 5 wt.% of PEG is excellent for achieving the desired performance in ultrafiltration. The membrane exhibits a notable removal efficiency of 99.5% when operated at a pressure of 6 bar.

Keywords: Composite UF membrane; Dye removal; PES polymer; PEG polymers

Received: 27 November; Revised: 04 December; Accepted: 11 December 2023

1. Introduction

Industrial wastewater is composed of various organic and inorganic pollutants, necessitating the implementation of purification processes before discharging into the environment. This includes the removal of dyes, among other toxins [1,3]. The visual impact of dyes in water, water clarity, and gas solubility in lakes, rivers, and other aquatic environments are significantly influenced by the presence of little quantities of dyes in water, often measuring less than 1 ppm for certain dyes [4]. These effluents' treatment methods commonly employed are chemical precipitation, activated sludge, chlorination, activated carbon adsorption, and membrane processes [5]. A wide range of methods have been developed to tackle this matter. The process of coagulation and flocculation [6], biological processing [7], enhanced oxidation [8-12], adsorption [13], and membrane processing [14].

membrane separation technology commonly used in several applications, such as water treatment and the treatment of dye-based wastewater, owing to its compact size, exceptional separation effectiveness, little energy requirements, and straightforward and secure operational procedures [15,16]. The membrane material is of greatest significance when calculating the separation performance, acting as the critical element of membrane separation technology [17,18]. This method offers several advantages, including reducing sludge, the absence of supplementary chemicals, the generation of consistent and high-quality permeate, a minimal spatial requirement, and ease of operation [19-22].

Flat sheet membranes are widely utilised in various industries, with a particular emphasis on wastewater treatment, owing to their notable attributes such as flexibility, simplicity, and commendable functional capabilities. Pressurized liquid filtration techniques, such as reverse osmosis (RO), nanofiltration (NF), ultrafiltration (UF), and microfiltration (MF), are extensively employed in the treatment of large volumes of contaminated water. Nonetheless, both reverse osmosis (RO) and nanofiltration (NF) technologies exhibit limited permeability, necessitating elevated pressure levels to mitigate this limitation, consequently leading to escalated processing expenses [22]. However, the UF and MF processes have low operating pressure and high water permeability relative to other membrane technologies, yielding reduced energy expenditure [23,24]. Polymeric membranes indicate a costeffective nature. although they possess asymmetrical configuration that leads to reduced surface porosity and permeability Polyethersulfone (PES) is a common material in the application of separation. PES and PES-based membranes have remarkable stability in terms of oxidation, heat resistance, hydrolysis resistance, and mechanical properties. The phase inversion method is utilized to fabricate membranes that consistently possess an asymmetrical structure. The ultimate structure of the membrane is influenced by various factors such as the composition of the PES solution (including concentration, solvent, and additives), temperature, the use of non-solvents or a combination of non-solvents, the environment or coagulation bath, and other relevant parameter [26].

This study involved using (PES) membranes to create ultrafiltration (UF) membranes by the phase inversion method, which showed excellent results. The present study examined the Malachite Green dye filtration efficiency of the PES/PEG composite UF membranes prepared at various parameters, including cross-sectional morphology, hydrophilicity, roughness, and water flux. The ultimate structure of the composite UF membranes was determined using Fourier transform infrared (FTIR), scanning electron microscopy (SEM), atomic force microscopy (AFM), and porosity analysis.

2. Materials and Method

Polyether sulfone (PES) with molecular weight 56,000 supplied by BASF company (USA) was used to prepare the membrane casting solutions. NN-Dimethylformamide (DMF, H.CO.N(CH₃)₂, and minimum assay 99%) was used as a solvent from Amber Nath (India). Poly ethylene glycol (PEG) with molecular weight 6,000 supplied by Himedia Laboratories Pvt. Ltd. (India) to grow pore size of membrane. Malachite green (MG) dye with chemical structure ($C_{23}H_{26}N_2Cl$) was supplied from Sigma-Aldrich (USA). The chemical formula of malachite green dye is shown in Fig. (1). Deionized (DI) water was used in the experiments.

Fig. (1) The structure of the malachite green dye

Using the phase inversion technique, a matrix of ultrafiltration membranes using 16 wt.% of PES with (0, 5, 10, and 15 wt.%) PEG polymers. Table (1) displays the chemical compositions of each casting solution. The casting solution was prepared for each of the membranes by solving a specific amount of PEG in the DMF. The casting solution was then magnetically agitated for 6 h after PES was added to the solutions and then magnetically agitated for 6 h. The casting solution was allowed to be degassed for 24 hours. On a clean glass, a (150) micrometer thickness of casting solution was applied using a casting Gardner knife (Filmography: film casting doctor blade). Glass and cast film were briefly submerged in DI water. In order to get rid of any remaining solvent, the created membrane floated off the glass surface. Before testing, membranes were maintained in DI water for at least 24 hours. Monitoring revealed that the process temperature was constant at 35°C.

The composition of ultrafiltration membranes was determined by measuring the FT-IR spectra of the samples using a spectrometer from PerkinElmer, Australia. To assess the surface roughness of the membrane, a scanning probe microscope (SPM AA300 Angstrom Advanced Inc., AFM, USA) was utilized. The membranes that had been created were sectioned into smaller square shapes and affixed onto a metallic substrate. A microscopic scale of one micron by one micron was employed to observe the surfaces of the membranes. The scanning of the membrane surface was conducted using a tapping mode, and all measurements were performed on membrane samples that had been dried under natural atmospheric conditions. A scanning electron microscopy (SEM) technique was utilized to examine the surface and cross-section morphology of membranes. The assessment of membrane porosity holds significant importance in various membrane applications, particularly in assessing the separation performance of membranes. To assess the porosity of flat sheet membranes, a representative sample of each membrane was subjected to a weighing process, followed by immersion in distilled water for a duration of 2 min. The sample's dry weight and wet weight were measured by recording its weight before and after water immersion, respectively. The percentage porosity of the flat sheet membranes was determined by employing the gravimetric method to calculate the overall porosity (ϵ), as indicated by the following equation [27]

$$\varepsilon = \frac{(w_1 - w_2)}{(A \times T \times d) \times 100} \tag{1}$$

where A is the membrane effective area (m^2), w_1 is the weight of the wet membrane (g/m^3), w_2 is the weight of the dry membrane (g/m^3), d is the water density (998 kg/m³ at 25°C), and T is the thickness of the membrane (m)

The results of three independent replications of each test were considered. The mechanical property of the membrane is an important aspect of the membrane's practical applications like reusability, handling, and anti-deformation capacity [28].

The performance of the produced ultrafiltration membranes was evaluated by evaluating pure water flux and dye removal. Figure (2) depicts the crossflow filtration system, which consists of a membrane cell with an effective surface area of 24 cm². The permeability and removal of dye via the membrane were examined at room temperature and pressures in the (6 bar). Equation (2) was used to compute the permeate flux

$$F = \frac{v}{(A \times t)} \tag{2}$$

where F is the flux rate (L/m².h), V is the volume of permeate (Ltr), A is the effective area (m²), and t is the filtration time (h)

The solute rejection R (%) was calculated using Eq. (3) as

$$R = \frac{(c_f - c_p)}{c_f \times 100} \tag{3}$$

where C_f and C_p represent, respectively, the concentrations (mg/L) in the feed and permeate solutions. An ultraviolet-visible spectrophotometer was used to calculate the dye's concentration

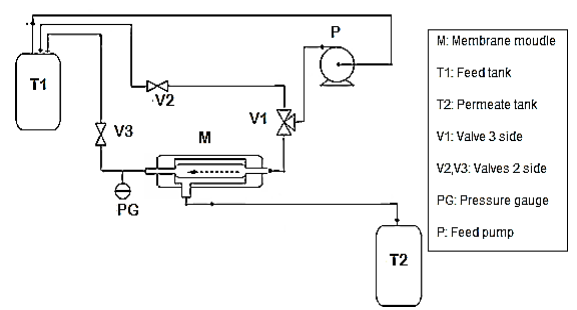


Fig. (2) A schematic diagram of the filtration system

3. Results and Discussion

The modification of surface composition in membrane is achieved through the utilization of FTIR-ATR spectrum analysis on the PES/PEG composite UF membranes, as represented in Fig. (4). It is noticeable that all of the samples have noticeable absorption spectra in the range 3700-3100 cm⁻¹. Figures (3a,b,c) depict the FTIR spectra of the membrane, wherein the membrane consists of pure, 5, and 10 wt.% of PEG, respectively. Three prominent absorptions are seen at 2967, 1585, 918, and 559 cm⁻¹, which correspond to the symmetric and asymmetric stretching vibrations of the COO- groups. Figure (3d) displays the FTIR spectrum of the membranes composed of Polyether sulfone (PES) blended with 15 wt.% PEG. The PEG absorptions exhibit significant peaks at 35027.3 cm⁻¹, as well as at 3394.72, 1627.92, and 950 cm⁻¹. The peaks around 3400 cm⁻¹ can be attributed to the presence of hydroxyl groups on the surface of the particles, which are typical in nature [29]. The presence of PEG in the composite membranes' structure was verified using FTIR spectroscopy. The peak corresponding to the stretch of PEG at 950 cm⁻¹ can be seen in all figures [30,31].

Figure (4) displays the surface and cross-sectional scanning electron microscopy (SEM) images of the PES membrane (Mu0) and the composite membranes with different quantities of PEG (Mu1, Mu2, Mu3, and Mu4). The SEM images of the fabricated membranes revealed a distinct asymmetric and porous structure featuring a prominently semi-dense skin layer, macro spaces, and a sub-layer with porosity. Despite the varied concentrations of PEG given, the cross-sectional observations of Mu1 to Mu3 were nearly identical due to the low concentration of the added PEG [32]. The PES membrane, in its original state, exhibits a characteristic structure resembling a sponge, as observed in the cross-sectional images. This morphology arises from the pronounced attraction between the non-solvent (water) and solvent (DMF), leading to rapid phase separation.

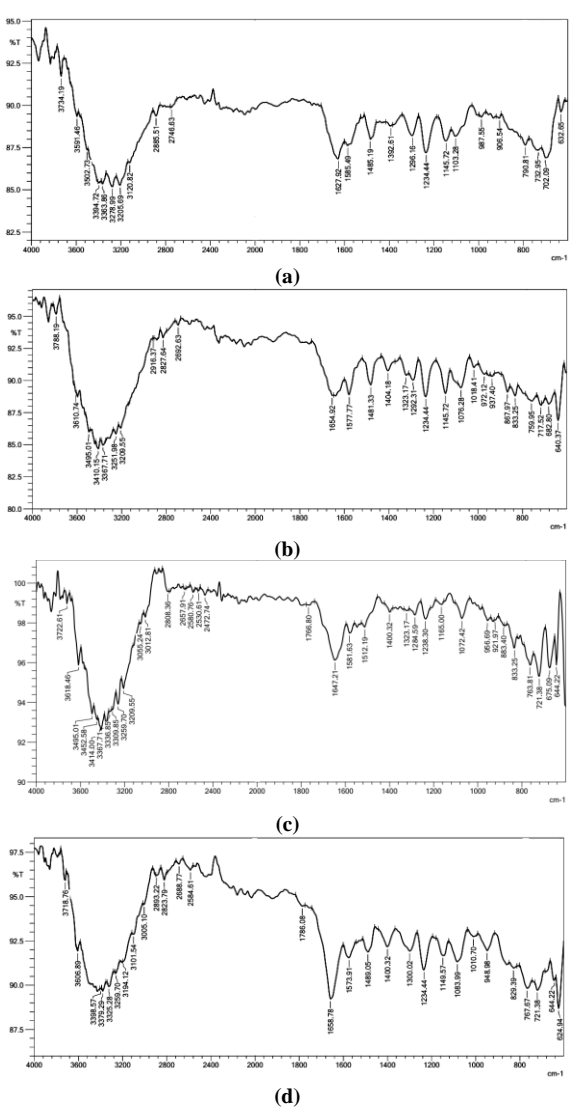
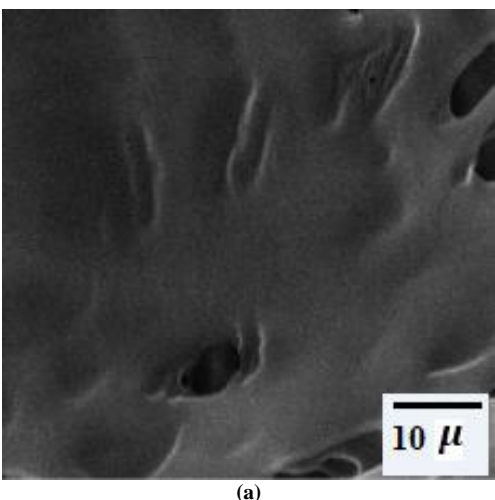


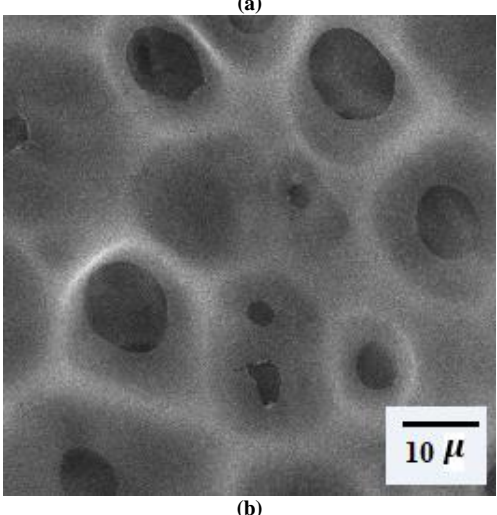
Fig. (3) FTIR-ATR spectra of (a) (0 wt.% PEG), (b) (5 wt.% PEG), (c) (10 wt.% PEG), and (d) (15 wt.% PEG) composite UF membranes

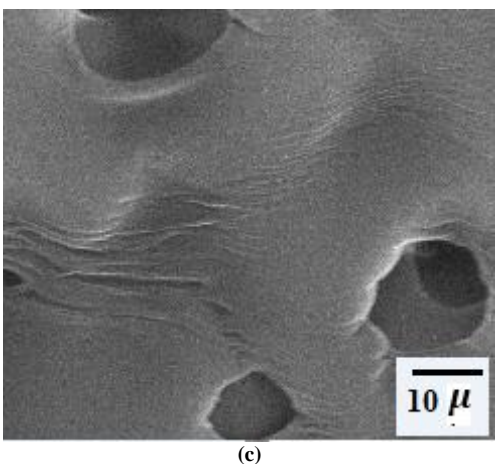
The addition of a hydrophilic PEG to the PES dope solution leads to a notable increase in the exchange rate between the solvent and non-solvent, as compared to the unmodified version. This is evidenced by the accelerated diffusion of water into the as-cast polymeric film. Subsequently, assuming a prominent role in initiating macro void formation and overall enhancement of porosity [33].

Furthermore, it was observed that the composite membranes exhibited a higher pore size compared to the pure PES membrane. The composite membranes showed enhanced connectivity of the perforations between the lower and upper layers, facilitating water transportation across the membrane, compared to the unmodified membrane. However, the addition of PEG enhances the membrane's permeability by increasing its porosity, expanding the size of the pores, and inducing the formation of some larger voids inside the skin layer. The macro gaps in the Mu2 and Mu3 membranes are most pronounced when the concentration of PEG is at its greatest. This

phenomenon has the potential to enhance water evaporation from the mixed matrix. The viscosity of the solution increases as the loading of PEG grows higher. The kinetics of the phase inversion process are influenced by the viscosity, leading to a reduction in the rate at which solvents and non-solvents exchange during the growth of membranes. The primary impediment to implementing structural modifications is the rate at which phase separation and solvent/non-solvent instantaneous demixing occur. These processes lead to an increase in density within the top layer of the membrane [34]. Despite the variations in the membrane structure caused by the increasing loading of PEG, the cross-sectional morphology remained comparable to that of the original PES.







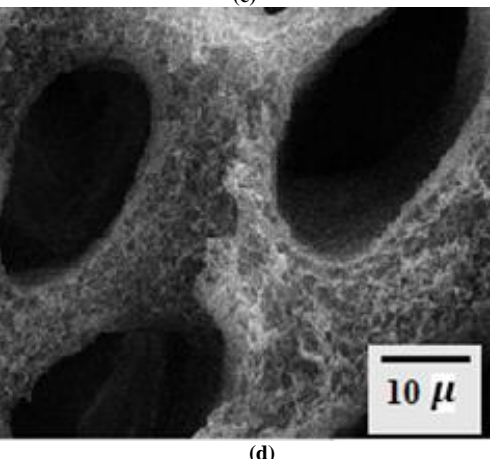


Fig. (4) SEM images of the surface of (a) 0 wt.% PEG, (b) 5 wt.% PEG, (c) 10 wt.% PEG, and (d) 15 wt.% PEG composite UF membranes

Table (1) examines the top surfaces of the PES membranes across a 4 cm² region to determine their porosity, and average roughness (Ra), which represents the average deviation of the surface from the centre plane. An observable correlation occurs between the concentration of PEG polymer and an increase in membrane porosity when demonstrated. In addition, the composite membranes showed higher porosity compared to the pure membrane. The porosity of the pure membrane is just slightly lower than that of the 5 wt.% PEG membrane, with values of 33.1% and 35.3%, respectively. Furthermore, the 10 wt.% PEG and 15 wt.% PEG membranes exhibited the greatest porosity, with values of 45.2% and 49.5%, respectively, leading to the formation of the largest macro-voids. Table (1) presents the surface roughness measurements. The surfaces of composite membranes were discovered to possess a somewhat more uneven texture compared to the original membranes. The increased surface roughness may be attributed to the accumulation of PEG polymers on the surface.

This behavior has been extensively documented by numerous studies, as indicated by references [35,36]. It is evident that when the proportion of PEG polymers increases, the average roughness of PES membranes likewise increases. This phenomenon can be attributed to the dimensions of the PEG polymer aggregates that have formed on the surface of the membrane. The surface roughness progressively increases from pure <5% PEG<10% PEG<15% PEG. Nevertheless, the presence of PEG polymers in the casting solution leads to a postponed blending of the liquid during the phase inversion process, hence causing an enlargement of the membrane's pore size. It is important to mention that the inclusion of PEG polymers resulted in an increase in both the average roughness of the membrane surface. The literature's accounts of this phenomena were in line with those presented in references [37,38].

Table (1) Profile roughness parameters and porosity of prepared membranes

Membrane	Porosity (%)	Average Roughness, Ra (nm)
0 wt.% PEG	33.1	24.81
5 wt.% PEG	35.3	81.65
10 wt.% PEG	45.2	96.53
15 wt.% PEG	49.5	102.5

The performance of membrane filtration and its operating lifetime are severely affected by the presence of membrane fouling. The reduction in membrane flux can be attributed to various factors. including the obstruction or occlusion of membrane pores, the occurrence of concentration polarization, and the creation of cake layers. A high-quality membrane should possess characteristics such as high flux, low fouling propensity, and sustained high rejection rate over an extended duration. The occurrence of membrane fouling can be attributed to a diverse range of underlying factors. The principal factor contributing to the inadequate antifouling performance is the hydrophobic nature shown by membrane surfaces [39]. Various strategies have been employed to enhance the hydrophilicity membranes, encompassing techniques such as material modification, polymer blending, and surface modification [40]. For improving the permeability of membranes and their resistance to fouling, some measures can be undertaken. The incorporation of hydrophilic polymer has been widely recognized as a highly effective and pragmatic approach for the development of antifouling membranes [41].

Figure (5) shows the significant increase of permeation flux through the three ultrafiltration (UF) membranes as a result of the MG dye filtration experiment. The addition of PEG greatly increases the flow. The use of PEG resulted in enhanced flow performance at pressures of 6 bar. By incorporating PEG polymer into the casting solution, the rate of mass transfer between the substrate and the coagulation bath increases during the phase inversion process. The addition of PEG enhances the membrane's porosity and water permeability, resulting in an increased water flux of an aqueous solution of MG dye. The flux rate of the three composite membranes the nearly linear flux curve.

Consequently, the reduced resistance to water flow in the membrane's interior during ultrafiltration is attributed to the formation of a larger quantity of interconnected pores, which in turn leads to an augmentation in water flow as the concentration of PEG increases. Conversely, a decrease in pore size on the selective surface of the membranes, specifically the outer surface in this case, may result in higher solute rejection [42].

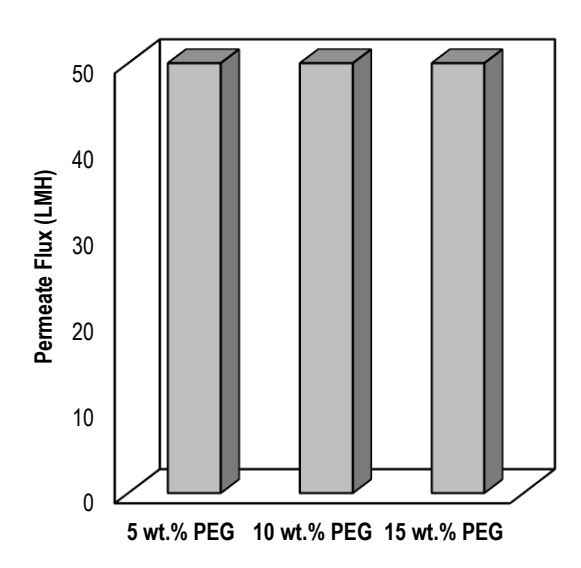


Fig. (5) Pure water Flux variations from aqueous solution of Malachite Green dye in composite ultrafiltration membranes under different (PEG) concentration

The assessment of the ultrafiltration performance of the manufactured membranes involved the utilization of MG dye. The cross-flow permeation test was employed to assess the dye rejection of the ultrafiltration membrane under operating pressures of 6 bar and a dye concentration of 10 ppm. Significant dye rejection was observed in all of the membranes that were generated. Ultrafiltration membranes frequently exhibit these behaviors. The efficacy of dye removal by the membranes is presented in the following order: the hypothesis is that the population means follow the order 0 PEG>5 wt.%>10 wt.% PEG. The observed decrease in rejection rates of the membranes with increasing concentrations of PEG indicates a significant increase in porosity, which can be related to the structural characteristics of the membranes. The inclusion of PEG in the polymer solution leads to an increased production of nuclei during the phase separation process. As the PEG concentration increases, the internal structure of the membranes becomes more relaxed, resulting in a decrease in hydraulic resistance for water transport across the membranes [42]. Figure (6) demonstrates the efficacy of commercially produced ultrafiltration (UF) membranes in the removal of Green dye from a solution of water. In comparison to the composite membranes 10 wt.% PEG and 15 wt.% PEG, the pristine membrane 0%PEG has a superior clearance efficiency. Although 15 wt.% PEG possesses the highest water permeability among all ultrafiltration (UF) membranes, it demonstrates the lowest level of dye loss when subjected to pressure. This phenomenon can be attributed to the permeability of water molecules and dye droplets through the membrane's surface.

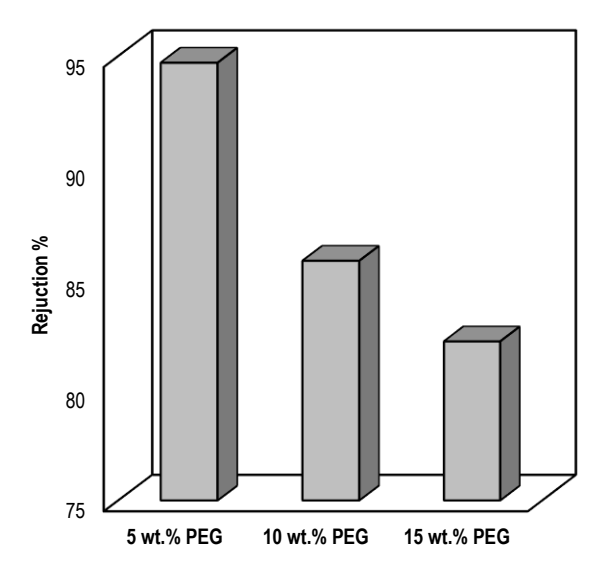


Fig. (6) Various removals for aqueous solution of Green dye in pristine and composite ultrafiltration membranes under different PEG concertation

The dye known as Malachite Green (MG) was solubilized in water at a concentration of 10 ppm, and the results of this experiment are depicted in Fig. (6). Both the 0.5 and 10 wt.% PEG membranes exhibited similar levels of dye rejection, with rejection rates of around 100% and 98% at a pressure of 6 bar, respectively. The 15 wt.% PEG membrane consistently exhibited the lowest rejection rate when subjected to the specified test pressure. Out of all the manufactured membranes, the 5 wt.% PEG membrane exhibits the most effective removal of dyes, with a complete clearance rate of 100% under a pressure of 6 bar specifically for the MG dye. The 15 wt.% PEG membrane enhanced hydrophilicity and reduced surface roughness are factors that might contribute to its higher rejection capabilities by minimizing foulant adsorption. Furthermore, it is commonly acknowledged that membranes exhibiting higher hydrophilicity tend to have a reduced propensity for fouling [43,44]. A compact hydration layer was generated to mitigate the adherence of dye droplets to the hydrophilic surface of composite membranes, which had absorbed a substantial amount of water molecules [45].

4. Conclusion

The pure water permeability of the composite membranes exhibited enhancement as the concentration of PEG increased, reaching a maximum

of 5 wt.%. Including PEG at concentrations of 10, 15, and 20 wt.% resulted in an augmentation in water permeability, mostly attributed to the corresponding rise in porosity. The permeability of the membranes exhibited an increase as the concentration of PEG rose, in contrast to the clean membrane. Malachite green dye (MG) removal efficiency, at a concentration of 5 ppm was found to be approximately 99.5% for all the membranes investigated. The composite membranes containing 15, 10, and 20 wt.% PEG exhibited a marginally reduced rejection rate compared to the unmodified pristine membrane. The composite membrane, with a content of 5 wt.% PEG, had the highest rejection rate. The composite membrane containing 5 wt.% PEG has optimum characteristics for the purpose of dye removal.

References

- [1] O.A.A. Mahmood and B.I. Waisi, "Synthesis and characterization of polyacrylonitrile based precursor beads for the removal of the dye malachite green from its aqueous solutions", *Desalin. Water Treat.*, 216 (2021) 445-455.
- [2] M.A. Mohammed et al., "Investigation the efficiency of emulsion liquid membrane process for malachite green dye separation from water", *Desalin. Water Treat.*, 307 (2023) 190-195.
- [3] I.S. Al-Bayati, S.A.M. Mohammed and S. Al-Anssari, "Recovery of Methyl Orange from Aqueous Solutions by Bulk Liquid Membrane Process Facilitated with Anionic Carrier", *AIP Conf. Proc.*, 2414 (2023) 1-7.
- [4] N.A. Mohammed, A.I. Alwared and M.S. Salman, "Photocatalytic Degradation of Reactive Yellow Dye in Wastewater using H₂O₂/TiO₂/UV Technique", *Iraqi J. Chem. Pet. Eng.*, 21(1) (2020) 15-21.
- [5] N. Mustafa and H. Al-Nakib, "Reverse Osmosis Polyamide Membrane for the Removal of Blue and Yellow Dye from Waste Water", *Iraqi J. Chem. Pet. Eng.*, 14(2) (2013) 49-55.
- [6] N. de C.L. Beluci et al., "Hybrid treatment of coagulation/flocculation process followed by ultrafiltration in TiO₂-modified membranes to improve the removal of reactive black 5 dye", *Sci. Total Environ.*, 664 (2019) 222-229.
- [7] A. Paz et al., "Biological treatment of model dyes and textile wastewaters", *Chemosphere*, 181 (2017) 168-177.
- [8] P.V. Nidheesh, M. Zhou and M.A. Oturan, "An overview on the removal of synthetic dyes from water by electrochemical advanced oxidation processes", *Chemosphere*, 197 (2018) 210-227.
- [9] O.A. Hammadi, F.J. Kadhim and E.A. Al-Oubidy, "Photocatalytic Activity of Nitrogen-Doped Titanium Dioxide Nanostructures Synthesized by DC Reactive Magnetron Sputtering Technique", Nonl. Opt. Quantum Opt., 51(1-2) (2019) 67-78.
- [10] F.J. Al-Maliki, O.A. Hammadi, B.T. Chiad and

- E.A. Al-Oubidy, "Enhanced photocatalytic activity of Ag-doped TiO₂ nanoparticles synthesized by DC Reactive Magnetron Co-Sputtering Technique", Opt. Quantum Electron., 52 (2020) 188.
- [11] F.J. Kadhim, O.A. Hammadi and N.H. Mutesher, "Photocatalytic activity of TiO₂/SiO₂ nanocomposites synthesized by reactive magnetron sputtering technique", J. Nanophot., 16(2) (2022) 026005 DOI: 10.1117/1.JNP.16.026005
- [12] Z.H. Zaidan, O.A. Hammadi and K.H. Mahmood, "Effect of Structural Phase on Photocatalytic Activity of Titanium Dioxide Nanoparticles", Iraqi J. Appl. Phys., 19(3A) (2023) 55-58.
- [13] C. Zhan et al., "Rice husk based nanocellulose scaffolds for highly efficient removal of heavy metal ions from contaminated water", *Environ. Sci. Water Res. Technol.*, 6(11) (2020) 3080-3090.
- [14] P.R. Sharma et al., "Nanocellulose-enabled membranes for water purification: perspectives", *Adv. Sustain. Syst.*, 4(5) (2020) 1900114.
- [15] J. Zhao et al., "Explorations of combined nonsolvent and thermally induced phase separation (N-TIPS) method for fabricating novel PVDF hollow fiber membranes using mixed diluents", *J. Memb. Sci.*, 572 (2018) 210-222.
- [16] M. Li et al., "Fractionation and concentration of high-salinity textile wastewater using an ultrapermeable sulfonated thin-film composite", *Environ. Sci. Technol.*, 51(16) (2017) 9252-9260.
- [17] Q. Zhang et al., "Loose nanofiltration membrane for dye/salt separation through interfacial polymerization with in-situ generated TiO₂ nanoparticles", *Appl. Surf. Sci.*, 410 (2017) 494-504
- [18] S. Alkarbouly and B. Waisi, "Dual-layer Antifouling Membrane of Electrospun PAN: PMMA Nonwoven Nanofibers for Oily Wastewater Treatment", Proc. 2nd Int. Multi-Discip. Conf. Theme: Integ. Sci. Technol., IMDC-IST 2021, 7-9 September 2021, Sakarya, Turkey (2022).
- [19] M. Tian et al., "Performance enhancement of ultrafiltration membrane via simple deposition of polymer-based modifiers", *J. Water Process Eng.*, 33 (2020) 1-7.
- [20] Z. Xu et al., "Antifouling polysulfone ultrafiltration membranes with pendent sulfonamide groups", *J. Memb. Sci.*, 548 (2018) 481-489.
- [21] D. Song et al., "Polysulfone/sulfonated polysulfone alloy membranes with an improved performance in processing mariculture wastewater", *Chem. Eng. J.*, 304 (2016) 882-889.
- [22] S.R.H. Abadi et al., "Ceramic membrane performance in microfiltration of oily wastewater", *Desalination*, 265(1-3) (2011) 222-

- 228.
- [23] S.M. Alkarbouly and B.I. Waisi, "Fabrication of Electrospun Nanofibers Membrane for Emulsified Oil Removal from Oily Wastewater", *Baghdad Sci. J.*, 19(6) (2022) 1238-1248.
- [24] Z.A. Khalaf and A.A. Hassan, "Studying of the effect of many parameters on a bulk liquid membrane and its opposition in Cd(II) removal from wastewater", *J. Phys. Conf. Ser.*, 1973(1) (2021) 012097.
- [25] L. Bukman et al., "Reverse micellar extraction of dyes based on fatty acids and recoverable organic solvents", Sep. Purif. Technol., 242 (2020) 116772.
- [26] C.L. Min, "High performance stainless steel-ceramic composite hollow fibres for microfiltration", *J. Memb. Sci.*, 541 (2017) 425-433
- [27] H.S. Al-Okaidy and B.I. Waisi, "The Effect of Electrospinning Parameters on Morphological and Mechanical Properties of PAN-based Nanofibers Membrane", *Baghdad Sci. J.*, 20(4) (2023) 1433-1441.
- [28] H. Sabeeh and B.I. Waisi, "Effect of Solvent Type on PAN–Based Nonwoven Nanofibers Membranes Characterizations", *Iraqi J. Chem. Pet. Eng.*, 23(4) (2022) 43-48.
- [29] Z.H. Zhou et al., "Nanocomposites of ZnFe2O4 in silica: synthesis, magnetic and optical properties", *Mater. Chem. Phys.*, 75(1-3) (2002) 181-185.
- [30] G.J. Copello et al., "Removal of dyes from water using chitosan hydrogel/SiO₂ and chitin hydrogel/SiO₂ hybrid materials obtained by the sol–gel method", *J. Hazard. Mater.*, 186(1) (2011) 932-939.
- [31] M.M. Hassan, Z.N. Abudi and M.H. Al-Furaiji, "Polysulfone Ultrafiltration Membranes Embedded with Silica Nanoparticles for Enhanced Dye Removal Performance", *Prog. Color. Color. Coatings*, 16(2) (2023) 165-179.
- [32] J.-F. Li et al., "Effect of TiO₂ nanoparticles on the surface morphology and performance of microporous PES membrane", *Appl. Surf. Sci.*, 255(9) (2009) 4725-4732.
- [33] A. Razmjou, J. Mansouri and V. Chen, "The effects of mechanical and chemical modification of TiO₂ nanoparticles on the surface chemistry, structure and fouling performance of PES ultrafiltration membranes", *J. Memb. Sci.*, 378(1-2) (2011) 73-84.
- [34] A. Idris, N.M. Zain and M.Y. Noordin, "Synthesis, characterization and performance of asymmetric polyethersulfone (PES) ultrafiltration membranes with polyethylene glycol of different molecular weights as additives", *Desalination*, 207(1-3) (2007) 324-339.
- [35] M.R. Kakar, M.O. Hamzah and J. Valentin, "A review on moisture damages of hot and warm mix asphalt and related investigations", *J. Clean.*

- Prod., 99 (2015) 39-58.
- [36] A.L. Ahmad et al., "Fouling evaluation of PES/ZnO mixed matrix hollow fiber membrane", *Desalination*, 403 (2017) 53-63.
- [37] A. Sotto et al., "Improved membrane structures for seawater desalination by studying the influence of sublayers", *Desalination*, 287 (2012) 317-325.
- [38] S. Rajesh et al., "Preparation, morphology, performance, and hydrophilicity studies of poly (amide-imide) incorporated cellulose acetate ultrafiltration membranes", *Ind. Eng. Chem. Res.*, 50(9) (2011) 5550-5564.
- [39] C.H. Koo et al., "Review of the effect of selected physicochemical factors on membrane fouling propensity based on fouling indices", *Desalination*, 287 (2012) 167-177.
- [40] R. Kumar et al., "Permeation, antifouling and desalination performance of TiO₂ nanotube incorporated PSf/CS blend membranes", *Desalination*, 316 (2013) 76-84.
- [41] L.Y. Ng et al., "Polymeric membranes incorporated with metal/metal oxide

- nanoparticles: A comprehensive review", *Desalination*, 308 (2013) 15-33.
- [42] A. Cui et al., "Effect of micro-sized SiO₂-particle on the performance of PVDF blend membranes via TIPS", *J. Memb. Sci.*, 360(1-2) (2010) 259-264
- [43] N.F. Shoparwe, T.A. Otitoju and A.L. Ahmad, "Fouling evaluation of polyethersulfone (PES)/sulfonated cation exchange resin (SCER) membrane for BSA separation", *J. Appl. Polym. Sci.*, 135(7) (2018) 45854.
- [44] M. Al-Furaiji et al., "Effect of polymer substrate on the performance of thin-film composite nanofiltration membranes", *Int. J. Polym. Anal. Charact.*, 27(5) (2022) 316-325.
- [45] A.L. Ahmad, T.A. Otitoju and B.S. Ooi, "Optimization of a high performance 3-aminopropyltriethoxysilane-silica impregnated polyethersulfone membrane using response surface methodology for ultrafiltration of synthetic oil-water emulsion", *J. Taiwan Inst. Chem. Eng.*, 93 (2018) 461-476.